

## Supplementary figures

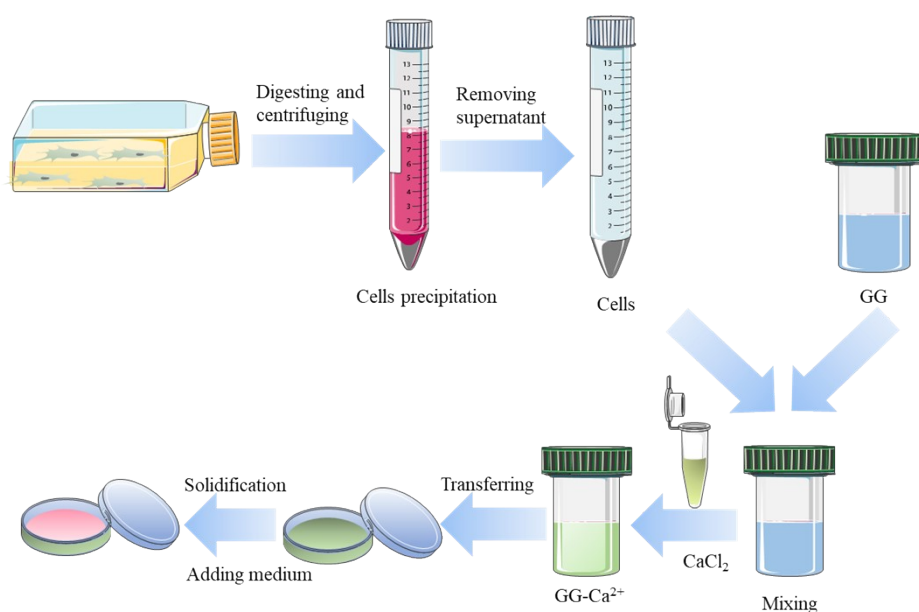


Figure S1. Schematic illustration of the process of 3D culture of bone marrow stromal cells (BMSCs) in gellan gum (GG).

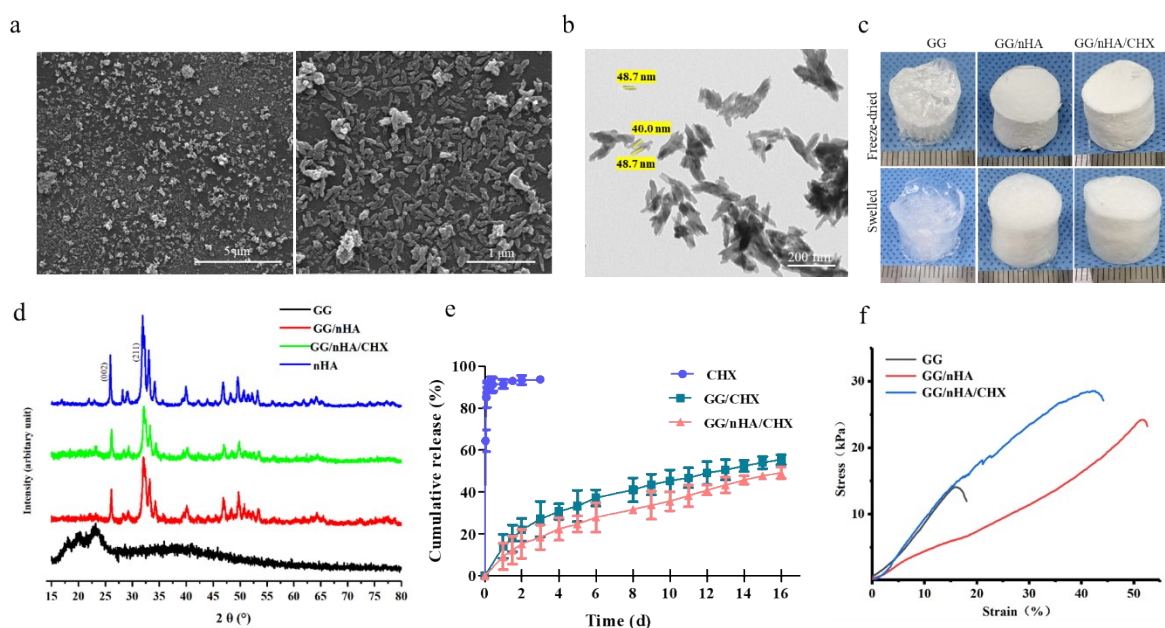


Figure S2. (a) SEM and (b) TEM images of nHA needle-like nanoparticles with sizes within 50 nm. (c) Photographs of swelled hydrogels. (d) X-ray diffraction pattern of the samples. (e) *In vitro* CHX release of hydrogels at 37 °C ( $n=3$ ). (f) Stress-strain curves of the samples.

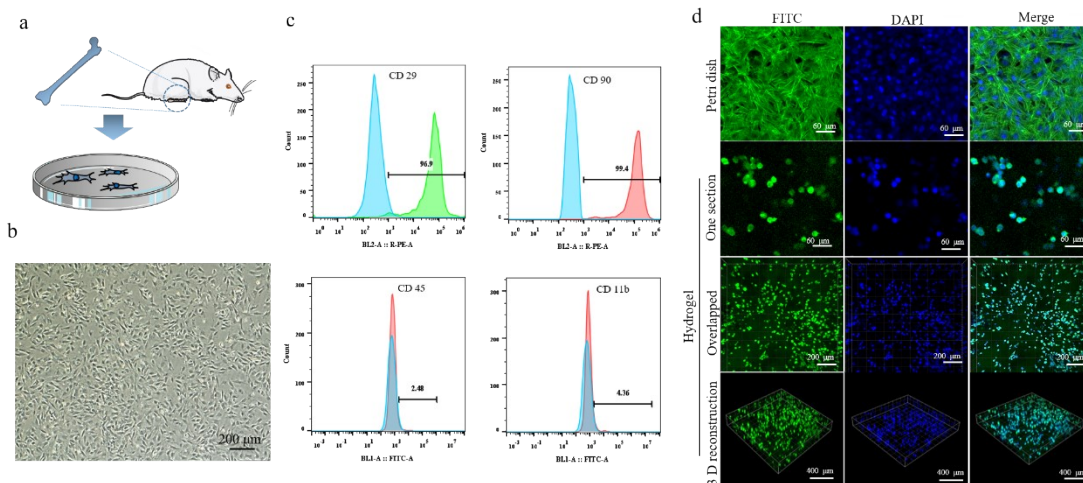


Figure S3. (a) Schematic illustration of the isolation of primary BMSCs obtained from rat femurs. (b) Morphology of third-generation BMSCs. (c) Percentages of CD29-, CD90-, CD45-, and CD11b-positive cells as detected by flow cytometry. (d) BMSCs were encapsulated in GG and stained with FITC-phalloidin. ‘Petri dish’ refers to BMSCs cultured on glass-bottom Petri dishes, ‘Hydrogel’ refers to 3D culture of BMSCs encapsulated in GG.

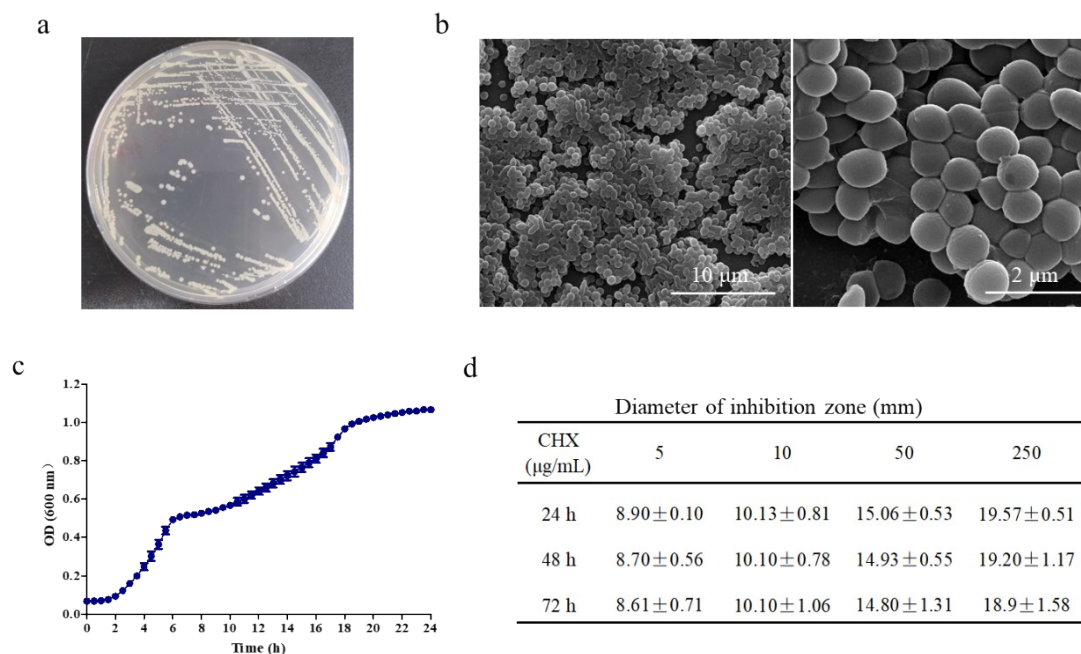


Figure S4. (a) Growth of *S. aureus* on LB agar medium. (b) Microscopic morphology of *S. aureus* as captured by SEM. (c) *S. aureus* growth curve for 24 h ( $n=5$ ). (d) Inhibition zone diameters measured using a Vernier calliper ( $n=3$ ).

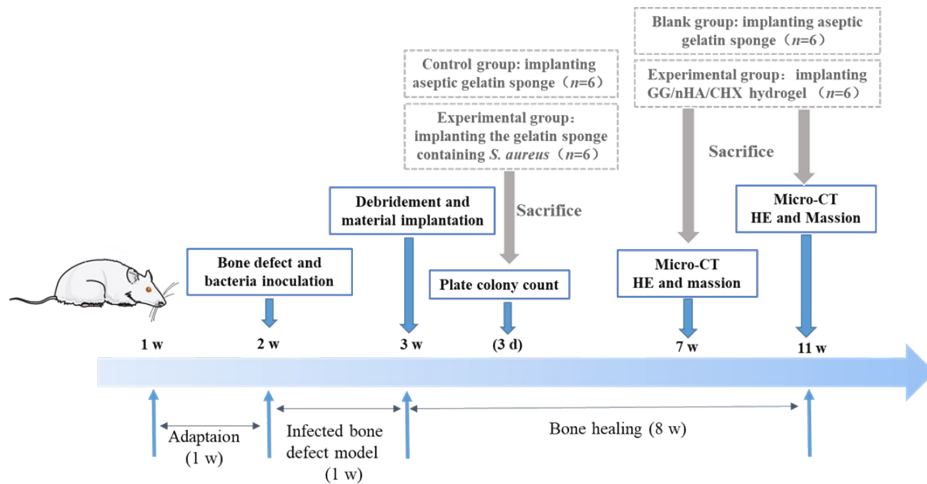


Figure S5. Workflow and timeline of the experiments to evaluate the antibacterial and osteogenic effects of the hydrogel *in vivo*.

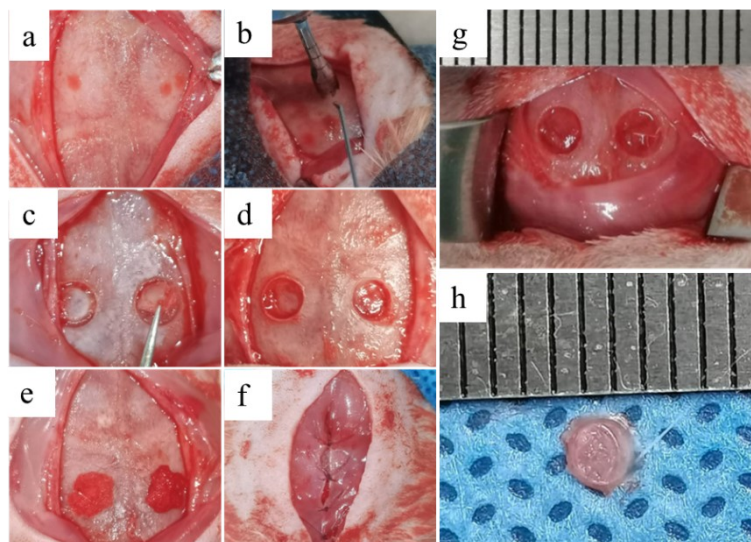


Figure S6. Photographs of the surgical procedure to create infected bone defects in rats. (a) Intraoperative view of exposing the coronal and lambdoid sutures of the cranium after incision of the skin and periosteum. (b) Defects were created with a trephine drill under saline irrigation. (c) Free bone fragments were carefully removed. (d) A full-thickness calvarial defect was created. (e) A sponge containing *S. aureus* was implanted in the defects. (f) The periosteum and skin were carefully sutured. (g, h) Two 3.0 mm-diameter symmetrical cranial defects were checked.